JCI The Journal of Clinical Investigation

Dietary carbohydrates regulate intestinal colonization and dissemination of *Klebsiella pneumoniae*

Aaron L. Hecht, … , Mark Goulian, Gary D. Wu

J Clin Invest. 2024. https://doi.org/10.1172/JCI174726.

Research In-Press Preview Gastroenterology

Graphical abstract

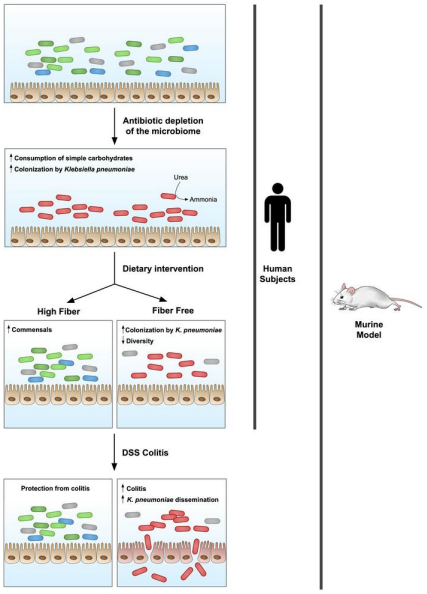

Dietary carbohydrates regulate intestinal colonization and dissemination of *Klebsiella pneumoniae*

Aaron L. Hecht[1#], Lisa C. Harling[1], Elliot S. Friedman[1], Ceylan Tanes[2], Junhee Lee[1], Jenni Firrman[3], Fuhua Hao[4], Vincent Tu[2], LinShu Liu[3], Andrew D. Patterson[4], Kyle Bittinger[2], Mark Goulian[5#], Gary D. Wu[1#]

[1]Division of Gastroenterology and Hepatology, Hospital of the University of Pennsylvania, Philadelphia, PA.

[2]Division of Gastroenterology, Hepatology, and Nutrition, The Children's Hospital of Philadelphia, Philadelphia, PA

[3]Dairy and Functional Foods Research Unit, Eastern Regional Research Center, Agricultural Research Service, US Department of Agriculture, Wyndmoor, PA.

[4]Department of Veterinary and Biomedical Sciences, Pennsylvania State University, University Park, PA 16802, USA

[5]Department of Biology, University of Pennsylvania, Philadelphia, PA

#Corresponding Authors:

Aaron Hecht: 936 BRB II/III, 421 Curie Blvd., Perelman School of Medicine, University of Pennsylvania, Philadelphia, Pennsylvania 19104, USA. Phone: 215-898-0158, Aaron.Hecht@pennmedicine.upenn.edu.

Mark Goulian: 204F Lynch Laboratory, Department of Biology, University of Pennsylvania, 433 South University Avenue, Philadelphia, PA, 19104, USA. Phone: 215-573-6991, goulian@sas.upenn.edu.

Gary D. Wu: 915 BRB II/III, 421 Curie Blvd., Perelman School of Medicine, University of Pennsylvania, Philadelphia, Pennsylvania 19104, USA. Phone: 215-898-0158 gdwu@pennmedicine.upenn.edu.

Conflict of Interest Statement

M.G. and G.D.W are inventors of the patent US 20160243175A1 entitled “Compositions and methods comprising a defined microbiome and methods thereof”.

The authors have no other interests to disclose.

Abstract

Bacterial translocation from the gut microbiota is a source of sepsis in susceptible patients. Previous work suggests that overgrowth of gut pathobionts, including *Klebsiella pneumoniae*, increases the risk of disseminated infection. Our data from a human dietary intervention study found that in the absence of fiber, *K. pneumoniae* bloomed during microbiota recovery from antibiotic treatment. We thus hypothesized that dietary nutrients directly support or suppress colonization of this gut pathobiont in the microbiota. Consistent with our human subject study, complex carbohydrates in dietary fiber suppressed colonization of *K. pneumoniae* and allowed for recovery of competing commensals in mouse modeling. In contrast, through ex-vivo and in vivo modeling, we identify simple carbohydrates as a limiting resource for *K. pneumoniae* in the gut. As proof of principle, supplementation with lactulose, a non-absorbed simple carbohydrate and an FDA approved therapy, increased colonization of *K. pneumoniae.* Disruption of the intestinal epithelium led to dissemination of *K. pneumoniae* into the bloodstream and liver, which was prevented by dietary fiber. Our results show that dietary simple and complex carbohydrates are critical not only in the regulation of pathobiont colonization but also disseminated infection, suggesting that targeted dietary interventions may offer a preventative strategy in high-risk patients.

Main Text

Introduction

Bacterial translocation from the gut microbiota is a significant source of sepsis in susceptible patients, including those with cirrhosis, acute myeloid leukemia, and intensive care unit admission (1–5). Dysbiosis, the altered microbiome associated with certain chronic conditions, is thought to perpetuate sepsis through selection for opportunistic pathogens and dysregulation of the immune response (6–11). This is often characterized by reduction of community diversity and the outgrowth of *Enterobacteriaceae*, including *Escherichia coli* and *Klebsiella pneumoniae* (6,8,12–

14). These organisms are commonly recovered in disseminated infections, including bacteremia and urinary tract infection, suggesting a connection with gut microbiota composition (15–18). Additionally, particular strains of *E. coli* and *K. pneumoniae* have been isolated from patients with inflammatory bowel disease (IBD) and cause more severe illness in animal models (19,20). Therefore, identification of mechanisms to increase colonization resistance against these opportunistic pathogens is essential.

Diet is a modifiable factor that is known to alter microbiota composition. Specified diets including elimination diet and Mediterranean diet have shown some clinical efficacy in the treatment of IBD, with improvement in dysbiotic signature (21,22), demonstrating that nutritional components have the potential to impact disease outcomes. Human gut microbiome response to diet is personalized, as it is dependent upon the pre-existing microbial population and dietary macronutrients (23–25). These macronutrients can directly affect the physiology of the resident microbiota by providing substrate for replication to organisms capable of utilizing them (26–28).

Two essential elements for growth of all bacterial species are carbon and nitrogen. Previous work suggests that nitrogen is a limiting resource for growth of organisms in the gut microbiome (29,30). Nitrogen is essential for anabolic processes including *de novo* synthesis of nucleotides and amino acids. Primary sources for nitrogen in the microbiota are dietary peptides, host-secreted digestive enzymes, glycoproteins from mucus, and the host-produced nitrogenous waste product urea, for which microbes have differing preferences (29,31). This can in turn affect host physiology, where an intact microbiota increases the daily requirement for host protein intake (32). Carbon sources are also critical for bacterial survival; in addition to providing carbon for anabolic pathways, these molecules serve as a primary source of ATP. Dietary simple carbohydrates and starches are predominantly metabolized and absorbed by the host in the small intestine, leaving low concentrations available to the microbiota in the colon. Non-digestible complex carbohydrates,

known as fiber, fall into the category of microbiota-accessible carbohydrates (MACs). The paucity of simple carbohydrates in the colon favors organisms capable of digesting dietary fibers through glycoside hydrolases (GHs) (26,27), conveying a significant effect on the microbiome in mouse and human studies (27,33). While *Bacteroidota* and *Bacillota* can ferment these complex carbohydrates (28), very little attention has been given to the impact of dietary MACs on *Enterobacteriaceae*, as their genomes have very low representation of genes encoding GHs necessary for their utilization (34).

We hypothesized that dietary nutrients affect colonization of *Enterobacteriaceae*. Through bacterial culture, ex-vivo studies, and mouse modeling we dissect the resource limitation of *K. pneumoniae*. Contrary to the commonly believed importance of nitrogen availability on the composition of the gut microbiota, we provide evidence that *Enterobacteriaceae* are not nitrogen limited but rather constrained by simple carbohydrate availability. Despite the growth promoting effects of simple carbohydrates on *Enterobacteriaceae*, we demonstrate in both a human dietary intervention study and mouse modeling that complex carbohydrates in fiber suppress colonization of *K. pneumoniae* and support the recovery of competitor commensals in the microbiota. Disruption of the intestinal epithelium induced systemic dissemination of this human pathogen, which was ameliorated by supplementation with dietary fiber. Our studies identify dietary factors critical for perpetuation and resolution of dysbiosis in the microbiome and resulting systemic disease.

Results

Fiber-free diet increases colonization of *K. pneumoniae* in a human study. A previously published study from our group examined the impact of dietary fiber on the microbial and metabolomic composition of the gut microbiome in human subjects, referred to as the Food and Resulting Microbial Metabolites (FARMM) study (33). Healthy human subjects were recruited, of

whom 20 normally adhere to a typical American diet (referred to as omnivore), and 10 to a vegan diet. The 20 omnivore subjects were randomized to a standardized omnivore diet or a fiber-free exclusive enteral nutrition (EEN) diet, while the vegan subjects remained on a vegan diet (**Figure 1A**). The omnivore and EEN diets were similar in macronutrient composition, except for the lack of dietary fiber in EEN and an altered ratio of saturated and unsaturated fats. After a five-day dietary phase, all participants were subjected to microbiota depletion via three days of nonabsorbable oral antibiotics (vancomycin and neomycin) together with a one-day polyethylene glycol (PEG) purge. Subsequent recovery of the microbiome was monitored via fecal analysis including shotgun metagenomic sequencing and metabolomics. Previously published results from this study revealed that the diet lacking in fiber, EEN, reduced microbial diversity during microbiome recovery and increased the relative abundance of *Pseudomonadota* (33), reminiscent of a dysbiotic signature.

Analysis of species abundance revealed that *K. pneumoniae* bloomed in the EEN group, accounting for over 50% of the microbiota, which was not observed durably in the omnivore and vegan groups (**Figure 1B; Supplemental Figure 1A**). There was a brief increase in abundance noted in the vegan group, which resolved by Day 13, correlating with the timing of microbiota recovery. At the final day of the trial, there was a clear separation of *K. pneumoniae* high (>20%) and low (<20%) subjects (**Supplemental Figure 1A**). Further analysis showed that *K. pneumoniae* high individuals had a distinct microbiota composition, but no consistent correlation with other organisms was identified (**Supplemental Figure 1B and C**). Prior to the initiation of the study, only one individual had detectable *K. pneumoniae* via shotgun sequencing, however, it is difficult to exclude the possibility that subjects were colonized at levels below the limit of detection by sequencing. These data suggest that an EEN diet provides a significant advantage to *K. pneumoniae* colonization during microbiota recovery.

One characteristic feature of *K. pneumoniae* is production of the enzyme urease, which metabolizes host-generated urea into ammonia, and has been associated with dysbiosis and inflammation in a mouse model of inflammatory bowel disease (35). We predicted that high abundance of *K. pneumoniae* would correlate with increased bacterial urease in the microbiome. Shotgun metagenomic sequencing confirmed an increase in the core urease genes in the EEN dietary group relative to the omnivore and vegan groups during microbiome recovery (**Supplemental Figure 2A**). Operon reconstruction found that the majority of urease is indeed attributable to *K. pneumoniae* in the EEN cohort (**Supplemental Figure 2B**). We additionally observed a spike of urease operon genes in the omnivore diet group during the early stage of microbiome recovery, which was found to be from *Streptococcus thermophilus* (**Supplemental Figure 2B**), likely attributable to its presence in yogurt in the omnivore diet.

Urea favors urease-encoding organisms in a complex microbial community. We hypothesized that *K. pneumoniae* colonization would alter the fecal nitrogen environment by metabolizing amino acids and urea into ammonia, thus providing a fitness advantage in colonization. During the dietary phase of the study, all 20 proteogenic amino acids are of low abundance (**Supplemental Figure 2C**). Antibiotic treatment increases stool amino acid levels, consistent with previously published study results (**Supplemental Figure 2C**) (33); however, during microbiome recovery, the EEN dietary group displayed decreased amino acid consumption relative to the omnivore and vegan groups on day 14 of the study (**Figure 1C**). Urea and ammonia quantification revealed that individuals with a high abundance of *K. pneumoniae* during microbiota recovery had decreased fecal urea and a corresponding increase in ammonia during microbiome recovery, while those with relatively low *K. pneumoniae* levels did not (**Figures 1D and E**). Thus, EEN supported higher levels of *K. pneumoniae* engraftment in human subjects and altered the luminal nitrogen composition of the microbiome.

We generated an in vitro model system to explore the role of urea in a complex gut microbial community. A bioreactor system was inoculated with a human fecal sample into two complex media: 1. Brain Heart Infusion (BHI) medium, in which the primary carbohydrate is glucose, or 2. SHIME medium, which contains complex glycans (36). The low concentration of urea in both media provided the opportunity to directly test the impact of urea on an intestinal microbial community. Samples were collected every 24 hours and subjected to shotgun metagenomic sequencing with relative species and gene abundances calculated. We found that in BHI, the addition of urea significantly increased the abundance of the urease-positive organisms *K. pneumoniae* and *Citrobacter freundii* (**Supplemental Figures 3A and B**). The abundance of urease genes accordingly increased with urea supplementation (**Supplemental Figure 3C**). These relationships were substantially diminished in SHIME media (**Supplemental Figures 3A-C**), supporting the theory that urease provides a growth advantage in the presence of urea through increased nitrogen availability only when a simple carbohydrate is available for use by *Enterobacteriaceae*.

Nitrogen is not a limiting resource for *K. pneumoniae* colonization in the gut. To rigorously test the hypothesis that nitrogen is growth limiting in the gut for *K. pneumoniae*, we generated two deletion mutants: the urease operon (△urease) and *ntrC* (△*ntrC*), which encodes a key regulator of the nitrogen scavenging Ntr system (37). While the WT strain grew well in vitro in an ammonia-limited environment with urea as an available nitrogen source, the △urease and △*ntrC* strains displayed delayed or limited growth (**Supplemental Figures 3D and E**). In an ammonia-rich environment, urea had no effect on the three strains. When tested on a range of nitrogen-containing compounds, the △*ntrC* strain was significantly restricted in its growth relative to the WT strain (**Supplemental Figure 4A**). Thus, we find that under nitrogen-limited environments in vitro, the *K. pneumoniae* has a broad capacity for nitrogen assimilation, dependent on urease and *ntrC*.

To directly test if restricting the nitrogen resources available to *K. pneumoniae* reduces colonization capacity in the gut, mice were colonized with WT, △urease, or △*ntrC K. pneumoniae* after antibiotic pre-treatment on a standard mouse chow (**Supplemental Figures 4C and D**). Interestingly, we found no colonization defect for the mutant strains, and in fact a previous study with *E. coli* observed a colonization advantage for a △*ntrC* mutant (38). These observations led us to speculate that under normal dietary conditions, the gut is abundant in available nitrogen. Previous work demonstrated that limitation of dietary protein significantly reduced ammonia and urea in the mouse intestine (39). However, we find that urease and *ntrC* are also dispensable for colonization of mice on a low-protein diet (**Supplemental Figures 4E and F**). The absence of complex carbohydrates similarly had no impact on colonization of △urease *K. pneumoniae* (**Supplemental Figures 4G and H**). We confirmed that urease did alter the intestinal nitrogen environment, increasing ammonia levels with corresponding urea consumption (**Supplemental Figure 4I-N**).

To rule out the effect of cross-feeding from other members of the microbiota on colonization of urease-null *K. pneumoniae*, we colonized germ-free (GF) mice with WT or △urease *K. pneumoniae*. Intestinal colonization of *K. pneumoniae* was independent of urease expression (**Figure 2A**). We found that, prior to gavage, fecal ammonia levels were remarkably low (**Figure 2B**), similar to that of microbiome depleted conventionally raised (CR) mice (**Supplemental Figure 4J**). Colonization with WT *K. pneumoniae* resulted in ~10-fold increase in fecal ammonia levels; this was partially urease-dependent as colonization with △urease *K. pneumoniae* resulted in significantly less ammonia production than the WT strain but remained ~4-fold above the GF baseline. WT *K. pneumoniae* colonization caused decreased fecal urea levels relative to the urease-deficient strain, demonstrating urea hydrolysis as a primary source of ammonia production (**Figure 2C**). Fecal amino acid analysis reveals a significant decrease in the concentration of several amino acids after colonization with the WT strain (**Figure 2D**), likely due to consumption

by *K. pneumoniae*. Combined with the production of gut ammonia by the △urease *K. pneumoniae* strain, this reduction of fecal amino acids suggests the utilization of amino acids as a carbon source via deamination, thereby leading to the release of ammonia into the luminal environment.

***K. pneumoniae* colonization is enhanced by increased carbon-source availability.** The observed pattern of amino acid consumption and ammonia production after *K. pneumoniae* colonization indicated that carbon may be the primary limited resource for *K. pneumoniae* colonization in the gut. Through in vitro testing, we found that *K. pneumoniae* has a strong preference for simple carbohydrates, in addition to select amino acids, and citric-acid cycle intermediates (**Supplemental Figure 4B**), while complex carbohydrates including inulin and dextrin are not utilized. Proton NMR quantification of fecal samples before and after colonization of GF mice identified several metabolites which were significantly reduced in concentration after *K. pneumoniae* colonization, including sucrose, pyruvate, and lactate (**Figure 2E**), all of which serve as carbon sources for *K. pneumoniae* in culture (**Supplemental Figure 4B**). These data support that *K. pneumoniae* is carbon limited in the intestinal environment, and that alternative sources of nitrogen are unnecessary for colonization.

The mammalian small intestine absorbs most simple carbohydrates and amino acids, supporting the hypothesis that *K. pneumoniae* is limited by carbon sources available in the colon. We generated an ex-vivo model in which the small intestinal or cecal contents of microbiota-depleted CR mice were extracted, sterilized, and used as culture media for growth of *K. pneumoniae*. Growth in the small intestinal extract was greater than that in the cecal content, suggesting that host-absorbed nutrients are important for intestinal growth of *K. pneumoniae*. Addition of the readily useable nitrogen source, ammonia, to cecal extract had no effect on growth of *K. pneumoniae*, however, glucose supplementation increased maximum density and growth rate (**Figures 2F and G**) to mirror that of the small intestinal extract.

One simple carbohydrate that is not absorbed or metabolized by the host is lactulose, an artificial disaccharide of galactose and fructose. We found that lactulose can be utilized as a sole-carbon source in minimal media for the tested strain of *K. pneumoniae* (**Supplemental Figure 4B**). We confirmed that addition of lactulose to ex-vivo cecal extract increased growth of *K. pneumoniae* measured by optical density and CFU (**Figures 2H and I**). Mice were provided lactulose in drinking water after colonization with WT *K. pneumoniae*. Compared to water control, lactulose increased *K. pneumoniae* colonization by 10-fold (**Figure 2J**). In total, these data provide strong evidence that colonization of *K. pneumoniae* in the gut microbiome is carbon restricted and that nitrogen is abundant in the intestinal environment.

Dietary fiber suppresses colonization of *K. pneumoniae* and supports commensal competitors. While available simple carbohydrates support the growth of *K. pneumoniae* in the gut, the majority of carbohydrates in the colon are complex and not absorbed by the host. We hypothesized that these complex carbohydrates, referred to as dietary fiber, may play a role in colonization resistance against *K. pneumoniae*. Indeed, results of the FARMM study demonstrate that the EEN diet, which is deficient in fiber, increased colonization of *K. pneumoniae* (**Figure 1B**). To test this hypothesis, we generated matched fiber-free (FF) and high-fiber (HF) mouse chows; the HF chow contained a well-characterized pea fiber (40). Groups of CR mice were provided FF or HF chow *ad libitum*, treated with the same oral antibiotic regimen provided to the FARMM subjects for three days to deplete the microbiota, and gavaged with *K. pneumoniae*. Calorie intake was equivalent between the groups, without significant differences in macronutrient consumption (**Supplemental Figure 5A**). As expected, we found that antibiotic treatment significantly reduced microbiome diversity when compared via shotgun sequencing (**Figure 3A**). During recovery, microbiome diversity was dependent upon dietary fiber, where the mice provided a HF diet returned to baseline diversity by 4 weeks and FF diet precluded such recovery. This

data mirrors that of the FARMM study, wherein human subjects on a fiber-free EEN diet did not recover to baseline diversity after microbiome depletion. PCoA analysis confirms that while antibiotic treatment significantly affects the community structure regardless of diet, the community on the FF diet remains persistently altered from baseline and the HF group (**Supplemental Figure 5B**). We hypothesized that fiber would enable asymmetric recovery of organisms encoding glycoside hydrolases (GHs) necessary for complex glycan metabolism. Indeed, while mice on a HF diet had increased levels of GHs enabling metabolism of plant-based carbohydrates, these were decreased in mice fed a FF diet (**Figure 3B, Supplemental Figure 6A**). In contrast, GHs for simple carbohydrates and animal glycans were disproportionately increased in the FF diet group, reminiscent of results from the FARMM study and consistent with the ability of a FF diet to select for a mucolytic community (41).

After gavage with *K. pneumoniae*, we found 1000-fold higher level of colonization in the FF group compared with the HF group (**Figure 3C**). Intriguingly, this difference only manifested after one week, corresponding with divergence in microbiome diversity between groups. Species analysis of the microbiome through shotgun metagenomics identified several organisms that were permanently lost on the FF diet, the recovery of which on a HF diet anti-correlated with *K. pneumoniae* (**Supplemental Figures 5C and D**). Several members of the microbiota including *Lactobacillus johnsonii*, *Bifidobacterium pseudolongum*, and a *Lachnoclostridium* species demonstrated a strong correlation with resistance to *K. pneumoniae* colonization (**Supplemental Figures 5C and D**), suggesting that these species may play a causative role in the effect of this dietary intervention. Analysis of metagenomic data from the FARMM trial found a similar pattern, in which *Lactobacillus* and *Bifidobacterium* species were at lower levels in the EEN dietary group compared with fiber-containing diets (**Supplemental Figure 6C**). Conversely, the pathobiont *Enterococcus faecalis,* was detected at high levels on the fiber-free diet four-weeks after antibiotic

treatment suggesting that these commensal strains may provide colonization resistance more broadly in the setting of dietary fiber.

Examination of the nitrogen composition of the gut demonstrated that stool ammonia is increased in the FF group, corresponding with higher levels of *K. pneumoniae,* and associated with urea depletion over the course of the study (**Figures 3D and E**). By contrast, we did not find such a relationship in the HF diet group (**Figures 3D and E; Supplemental Figure 6B**) similar to the results of the FARMM study (**Figures 1D and E**). Moreover, we observed higher levels of stool amino acids in the FF group relative to the HF group during microbiome recovery (**Figure 3F**), suggesting that organisms abundant on the HF diet preferentially consume amino acids. In summary, we have replicated several key features of the human subject FARMM study through mouse modeling by removing dietary fiber, including altered microbiome diversity, GH abundance, *K. pneumoniae* colonization, and nitrogen composition. Our results demonstrate that complex dietary carbohydrates play a key role in colonization resistance against *K. pneumoniae*.

Dietary fiber reduces bacterial dissemination after intestinal barrier disruption. To test the impact of dietary fiber on bacterial translocation, mice were colonized with *K. pneumoniae* on a FF or HF diet after antibiotic pre-treatment. After stable engraftment, mice were treated with dextran sodium sulfate (DSS) to induce intestinal inflammation and disrupt the epithelial barrier (**Figure 4A**). Consistent with previous studies, we found that disease activity, weight loss, and colon length were improved by the addition of dietary fiber (**Figures 4B-D**) (42,43). Colon histopathology revealed a concordant reduction in inflammation score in the HF group (**Figure 4E**). After four days of treatment, mice were euthanized and *K. pneumoniae* quantified from sections of the intestinal tract, liver, and blood. Dietary fiber not only reduced colonization of *K. pneumoniae* in the colon, but also in the proximal and distal small intestine (**Figures 4F-H**). We observed that fiber prevented dissemination of *K. pneumoniae* to the liver and blood, while mice

treated with an FF diet had greater levels of bacteremia and liver infection (**Figures 4I and J**). In total, our data unveil a novel role for dietary carbohydrates on colonization of *K. pneumoniae* in the gut and provide a possible treatment to reduce dissemination of this human pathogen.

Discussion

Dysbiosis is an important feature of many chronic diseases and involves the outgrowth of *Enterobacteriaceae* in the gut. Intestinal colonization of *K. pneumoniae* and other *Enterobacteriaceae* are thought to play a role in IBD and disseminated infectious diseases including bacteremia, cholangitis, and urinary tract infections. Identifying dietary components contributing to the formation and resolution of dysbiosis is therefore critical. Herein, we find that diet can have a direct effect on colonization of *K. pneumoniae* by serving as a nutrient source and an indirect effect via colonization resistance. Understanding the dietary resources necessary for colonization of harmful strains of *Enterobacteriaceae* could serve as a critical tool in targeted prebiotic interventions to prevent and/or treat disease.

Since both nitrogen and carbon sources are critical for bacterial growth and the environment of the distal gut is known to be a nutrient constrained environment (28), we systematically determined the relative importance of nitrogen- vs. carbon-based nutrients in the colonization of *Enterobacteriaceae* in both the murine and human gastrointestinal tract. Previous literature suggests that nitrogen is a limiting resource for bacterial growth in the mammalian gut (29,30). Urea is a host-produced nitrogenous waste product which is in turn excreted into the intestinal lumen and has long been speculated to be an important source of nitrogen for the microbiome, accessed via bacterial urease (28,44). Recent literature shows that bacterial urease is important for cross-feeding of nitrogen to non-urease encoding species (31). Our human subject and bioreactor data suggested that urease may be advantageous for the growth of *K. pneumoniae* in microbiome recovery, specifically when levels of the readily accessible nitrogen source, ammonia,

is less abundant. However, after rigorous testing in vitro, ex-vivo, and in vivo, we found that nitrogen is not a limiting resource for the colonization of *K. pneumoniae*. Even under nitrogen-starved conditions, bacterial urease and the nitrogen scavenging system, Ntr, are dispensable for growth of *K. pneumoniae*. Intriguingly, the presence of oligosaccharides correlates with a diminished effect of urea on the microbial composition in complex media. Determining if these carbohydrates mediate the nitrogen effect observed will require further studies, given the many differences between these complex medias with limited characterization. Overall, our data suggest that nitrogen is abundant in the mouse intestinal tract and that other dietary factors are more central for the colonization of this human pathogen.

Regardless, *K. pneumoniae* colonization has a significant impact on the nitrogen environment of the intestine. Only select amino acids are consumed after *K. pneumoniae* mono-association of GF mice, including serine and threonine, which are most likely being metabolized as carbon sources through deamination. *K. pneumoniae* colonized GF mice maintain higher levels of many amino acids compared to CR mice or humans with intact microbiota; other members of the community, particularly *Clostridia*, are capable of Stickland fermentation and thus have a broader accessibility to energy extraction from amino acids (45). Interestingly, we find that luminal ammonia, which serves as a preferred nitrogen source for most bacterial species, is dependent on the presence of the gut microbiome, where feces of GF mice, and antibiotic-treated mice and humans contain substantially lower levels. Our work demonstrates that while urease is a factor in ammonia production during colonization of GF mice, ammonia is also released from other sources, likely including amino acid deamination (46). While our conclusion regarding nitrogen abundance is limited to *K. pneumoniae*, it is plausible that other bacterial species in the gut microbiome are also nitrogen limited (28).

In contrast to our findings with nitrogen availability, our studies show that carbon sources are a major limiting factor for growth of *K. pneumoniae* in the gut. The host absorbs most simple carbohydrates in the small intestine, leaving a relative paucity of dietary simple carbohydrates available to the microbiota in the colon (47–49). Previous work focused on *E. coli* has identified multiple carbohydrate utilization genes important for competitive colonization of the GI tract, including gluconate, mannose, fucose, and ribose (50), thought to be liberated from host mucus polysaccharides (51). While *K. pneumoniae* carbohydrate consumption in the intestine is less well studied, recent work demonstrated that fucose utilization is important for intestinal colonization (52). The role of dietary carbohydrates in colonization of *Enterobacteriaceae* has previously not been well characterized. Our ex-vivo modeling reveals that growth in small intestinal luminal extract was greater than that of cecal extract, the effect of which was diminished with the addition of a simple carbohydrate to the cecal material. Host absorption of simple carbohydrates in the small intestine may limit their impact on the colonization of *Enterobacteriaceae* in the colon. However, supplementation of diet with a non-absorbed carbohydrate, lactulose, in a mouse model increased colonization of *K. pneumoniae*, consistent with the hypothesis that carbohydrates are a major limiting resource for colonization.

In contrast to simple carbohydrates, we find that complex carbohydrates in dietary fiber suppress colonization of *K. pneumoniae* both in humans and in mice correlating with increased microbiome diversity. Intriguingly, we find that the vegan and omnivore groups in the FARMM trial lack a sustained difference in *K. pneumoniae* colonization, despite evidence that the vegan subjects had higher dietary fiber intake (33). Thus, a dose-dependent response to dietary fiber is not clearly seen for *K. pneumoniae* colonization resistance. Two non-mutually exclusive hypotheses may explain this phenotype. First, it is plausible that dietary fiber reaches a threshold whereby above a particular quantity, the effect of increased fiber diminishes. Indeed, previous human studies support this concept (53–55). Second, the effect of fiber is personalized, dependent on the fiber-

type and baseline microbiota, which also has support from a previous clinical trial (56). Future work will be necessary to clarify the intersubject variability observed in response to fiber.

Consistent with the FARMM study, dietary fiber was associated with an enrichment for plant-based GH abundance in the fecal microbiome, whereas a fiber-free diet favored GHs for simple carbohydrates and animal glycans (33). Short chain fatty acids (SCFAs), often produced in the intestine from dietary fiber, have been shown to suppress *K. pneumoniae* growth via intracellular acidification (57). This suggests that dietary fiber may have two roles in inhibiting *Enterobacteriaceae* colonization: directly through SCFA production and by supporting the recovery of competing organisms encoding plant saccharide GHs. *Clostridioides difficile* colonization is somewhat analogous, as it also relies on both depletion of microbiome diversity and decreased SCFA production (58). Our results show that fiber not only impacts colonization of *K. pneumoniae* in the colon, but also in the proximal and distal small intestine during DSS colitis. As a member of the *Enterobacteriaceae* family, the relatively bile and oxygen rich environment of the small intestine is likely to favor *K. pneumoniae* growth (59). This finding could have been influenced by coprophagia, however, which has been shown to significantly alter small intestinal microbiota composition in mice (60). Further studies will be necessary to define the causal strain(s), the essential GHs, and the role of coprophagia in this phenotype.

The suppression of *K. pneumoniae* colonization in the microbiome may have significant disease implications. For patients with IBD, reducing *K. pneumoniae* colonization improved host inflammatory response (20). Moreover, disseminated *K. pneumoniae* infections, in part, derive from the gut microbiome (61). Indeed, we find that disruption of the intestinal barrier with DSS leads to dissemination of *K. pneumoniae* to the liver and bloodstream, which is nearly eliminated by reduction of colonization with dietary fiber. Lack of fiber in the diet has separately been shown to increase the severity of DSS and infectious colitis, and thus the effect observed is likely

multifactorial (41,42). The impact of fiber on IBD has been the subject of significant controversy, with evidence demonstrating both benefits and risks associated with complex carbohydrate supplementation for these patients. Several recent studies in humans and mice suggest that the effect of fiber on inflammation is carbohydrate, microbiota, and model-dependent (56,62,63). While our data show a role for dietary fiber in the suppression of acute colitis, future work will be required to demonstrate if this is applicable to chronic inflammation.

Our studies reveal the critical importance of dietary carbohydrates in colonization of *K. pneumoniae* in the mammalian gut. This work may have direct relevance to human disease; patients hospitalized in the intensive care unit often require EEN as their sole source of nutrition, which is typically given without fiber supplementation. The outgrowth of *Enterobacteriaceae* in this setting due to poor microbiome diversity may predispose these patients to disseminated infection. Resolution of dysbiosis through rational prebiotic and probiotic therapies would have a range of therapeutic applications. Understanding the limiting metabolic resource(s) for these disease-associated organisms and the impact of diet on their colonization is a key step in designing such treatment strategies.

Methods

Sex as a biological variable

Our human study examined both male and female subjects, and combined findings are presented in the manuscript where there was no significant difference in the results between male and females. The mouse modeling was conducted in female mice only to reduce variability and because results are expected to be relevant regardless of biological sex based on the results of our human study.

Bacterial strains, culture conditions, and antibiotics

K. pneumoniae strain used was MGH 78578, as noted in Supplemental Table 1. *K. pneumoniae* was grown in LB (miller) medium aerobically at 37°C unless otherwise noted. M9 minimal media was used with carbohydrate or nitrogen supplementation as follows: 0.1% ammonia, 0.2% glucose, or 0.2% lactulose where noted. Antibiotics used were as follows: kanamycin, apramycin, vancomycin, and hygromycin at concentrations of 25, 100, 8, and 50μg/mL, respectively.

Strain Construction

Deletion of indicated genes in the MGH 78578 *K. pneumoniae* strain was performed via Recombineering through replacement of the targeted with a FRT-apramycin-FRT construct and subsequent excision, as previously described (64). In brief, the pMDIAI plasmid served as the template for PCR amplification of the apramycin resistance cassette, flanked by FRT sites and a 50bp overlap region with the target gene. Electrocompetent *K. pneumoniae* was transformed with pACBSR-hyg for Recombineering (65). The PCR amplified cassette was purified and electroporated into this strain with 1μg of DNA and plated on LB-apramycin. The pFLP-hygromycin plasmid was used to excise the antibiotic resistance cassette and all plasmids were cured from the strain through serial growth. PCR confirmed the mutant strains. See Supplemental Tables 1 and 2 for plasmid information and oligonucleotide sequences.

Nitrogen and Carbon Sources Analysis

To determine sole carbon and nitrogen sources available to *K. pneumoniae*, the WT or △*ntrC* strains were growth overnight in M9 minimal media with ammonia and glucose, washed in PBS, diluted 1:1000 into M9 minimal media without ammonia (nitrogen testing) or without glucose (carbon testing). Overnight grown culture was diluted 1:1000 in sterile PBS and was aliquoted into Biolog Phenotype microarray 96-well plates PM1, PM2A (carbon testing), and PM3B (nitrogen testing). OD_{600} was determined via BioTek Epoch2 plate reader, grown for 24 hours

shaking at 37°C. Area under the curve was calculated with software Prism v9.5.1 after subtracting background absorbance.

Bioreactor model

Eppendorf (Hamburg, Germany) Bioflo 320 bioreactors were assembled according to the manufacturer's specifications. During the experiment, all bioreactors were maintained at a temperature of 37 °C with agitation set to 100 rpm. The pH was kept at 7 ± 0.1, using 1 M NaOH and CO_2 gas. There was a constant sparging of gas at a rate of 1L/min, with the ratio of N_2:CO_2 dependent on the pH control. The initial volume of the bioreactors was 750 mL of either Brain Heart Infusion (BHI) broth) or a 70:30 ratio of Adult M-SHIME® growth medium:Pancreatic Juice. Adult M-SHIME® growth medium with starch was purchased from ProDigest (Ghent, Belgium) and consists of arabinogalactan (1.2 g/L), pectin (2 g/L), xylan (0.5 g/L), glucose (0.4 g/L), mucin (2 g/L), and starch (4 g/L), as well as yeast extract (3 g/L) and peptone (1 g/L) which provide nitrogen and trace nutrients (66). Pancreatic juice was made fresh every 2-3 days and contained 12.5 g $NaHCO_3$ (Sigma-Aldrich, St. Louis, MO), 6 g oxgall bile (Becton-Dickinson, Franklin Lakes,NJ) and 0.9 g pancreatin (Sigma-Aldrich, St. Louis, MO) (36). The bioreactors were connected using silicon tubing (Cole Parmer, Vernon Hills, Il) to a supply of medium and pancreatic juice to provide nutrition and biliary-pancreatic enzymes and to a bard urinary drainage bag (Becton, Dickinson and Company, Franklin Lakes, NJ) to collect waste. For inoculation, fecal samples were suspended at 10% wt/v in phosphate buffer within an anaerobic chamber. Buffer consisted of 0.8 g K_2HPO_4, 6.8 g KH_2PO_4, 0.1 g Sodium thioglycolate, 15 mg sodium thionite per liter with pH adjusted to 7. At time of inoculation, 10 mL of fluid was removed from the bioreactor and 10 mL of the resuspended inoculums added. The bioreactors were grown overnight, 16h, with temperature, pH, agitation, and gas flow. Following overnight growth, the bioreactors were maintained with daily feeding cycles in which the bioreactor was provided fresh medium and pancreatic juice. Every 8 h, the volume of the bioreactor was reduced to 600 mL and 150 mL of

either fresh BHI or a 70:30 Adult M-SHIME® growth medium:Pancreatic Juice mixture was added. Residence time was 40 h.

Reactors were inoculated with a baseline fecal samples from a healthy human subject enrolled in a previously described dietary intervention study (33). Following a 14-day period at baseline conditions, urea was supplemented to the feed at a concentration of 10 mM for an additional 14-day period. Samples were collected in the morning prior to the beginning of the feeding cycle.

Human Subjects

Stocked fecal samples from a previously reported human study called Food and Resulting Microbial Metabolites (FARMM) were tested where noted (33). In brief, the FARMM study consisted of 30 healthy human subjects, 10 of whom were vegan at baseline, 20 of whom had a typical Western (omnivore) diet. Vegan subjects maintained an outpatient vegan diet during the study. The omnivore group were randomized to a standardized omnivore diet or exclusive enteral nutrition (EEN) diet, consisting of Modulen® IBD. The omnivore standardized diet was designed to have similar composition, excepting the lack of dietary fiber in EEN. All subjects underwent three days of oral vancomycin 500mg and neomycin 1000mg every 6 hours on days 6, 7, and 8 of the study. All subjects were also given a bowel purge consisting of 4L polyethylene glycol purgative (GoLytely®).

Mice

SPF C57Bl/6J female mice were purchased from Jackson Laboratories at 8 weeks of age. Mice were housed under standard lighting cycle conditions (12 hours on/12 hours off) and provided acidified water. There was no investigator blinding for these studies and no animals were excluded from analysis.

Mouse *K. pneumoniae* Colonization Model

All CR mice were specific pathogen free (SPF) C57Bl/6J strain females acquired from Jackson Laboratories at 8 weeks of age. For colonization with *K. pneumoniae*, mice were treated with the antibiotics vancomycin (2.5g/L) and neomycin (5g/L) with aspartame (25g/L) in the drinking water provided *ad libitum* for 72 hours. Mice were then orogastrically gavaged once with 10^8 CFU of *K. pneumoniae* in 100µL, the inoculum of which was generated from aerobically grown overnight culture in LB media, washed and diluted 1:10 in sterile PBS. Fecal samples for CFU analysis were collected, homogenized in PBS, serially diluted, and spot plated on LB agar supplemented with kanamycin and vancomycin, or MacConkey agar supplemented with kanamycin, vancomycin, and tetracycline. Plates were incubated for 12 hours at 37°C, colonies counted, and CFU calculated per weight of fecal sample. C57Bl6/J mice from Jackson Laboratories have been previously shown to not be colonized with *Enterobacteriaceae* at baseline, which limits background signal via this method (67). Prior to and after antibiotic treatment, but before gavage, each mouse is routinely tested for resistant colonies.

Fecal samples collected for metabolomics analysis were flash frozen in dry ice and stored at -80℃. Diets were irradiated and provided *ad libitum*; the following diets were used in the indicated experiments: standard diet (Research Diets, AIN-76A), fiber-free diet (TestDiet 5Z6G), high fiber diet (TestDiet 5Z6L; containing Vitacel Pea Fiber EF-100 from J. Rettenmaier, USA), and low protein diet (Research Diets, D08092201).

For lactulose treatment experiments, mice were colonized with *K. pneumoniae* and subsequently provided 5% lactulose w/v in drinking water *ad libitum* after two weeks of colonization.

Mouse DSS and Dissemination Model

For DSS colitis model, mice were treated with 5% DSS in the drinking water. Mice were monitored for disease activity, similar to previously published protocols (68). In brief, mice were scored daily on the criteria outlined in **Supplemental Table 3**. The scores of each subsection were summed to provide a total daily score for each mouse, for a maximum daily score of 12. After four days of

treatment, mice were euthanized, and liver and blood harvested. Luminal content was collected at the time of euthanasia from the proximal 10cm of small intestinal, distal 10cm of small intestine, and fecal pellets. Colon length was measured at the time of euthanasia. Liver samples and intestinal luminal contents were homogenized and all samples were serially diluted and spot plated for CFU on LB with kanamycin and vancomycin. CFU were calculated per weight or per liver, as indicated.

For evaluation of colonic microscopic inflammation after DSS treatment, colonic tissue was dissected, opened on the anti-mesenteric margin, and Swiss-rolled. The tissue underwent fixation in 10% formalin for 24 hours and washed and stored in 70% ethanol. Tissue was paraffin embedded, sectioned, and hematoxylin and eosin stained. Tissue sections were evaluated for inflammation by an independent pathologist in a blinded fashion, using a modified scoring system from previous literature (**Supplemental Table 4**) (69,70).

Germ Free Mouse Colonization Model

For germ-free animal experiments, C57Bl/6J female mice were raised and maintained in sterile conditions in the University of Pennsylvania Gnotobiotic Facility. For colonization, mice were orogastrically gavaged at 8-weeks of age with indicated *K. pneumoniae* strains. Fecal samples were harvested before and after gavage at indicated time points and subjected to noted CFU and metabolomics analysis.

Ex vivo model

C57Bl/6J female mice 8 weeks of age were obtained from Jackson Laboratories and treated with antibiotics as previously noted for 72 and the final 24 hours with 10% polyethylene glycol in the drinking water. Regular water was then resumed for 24 hours. Mice were then euthanized and small intestinal or cecal luminal content was harvested, weighed, and resuspended in M9 minimal media without ammonia or glucose supplementation at a ratio of 4mL:1g material. Samples were

homogenized for 10 minutes and centrifuged at 10,000 x g for 10 minutes twice. Supernatant was filter sterilized through syringe driven 0.45μm PTFE filter. For aerobic experiments, overnight aerobic culture of *K. pneumoniae* grown in LB was washed in PBS, diluted 1:1000, and inoculated into 200μL of SI or cecal extract in 96 well plates. For anaerobic experiments, SI or cecal extracts were allowed to equilibrate in anaerobic chamber for 24 hours and inoculated with PBS-washed anaerobic overnight culture of *K. pneumoniae*, diluted 1:1000. Growth was monitored for 24 hours via OD_{600} in BioTek Epoch2 plate reader, incubated at 37°C. CFU was obtained via serial dilution and spot plating on LB agar with kanamycin and vancomycin after 24 hours of growth.

Shotgun Sequencing and Analysis

DNA was extracted from stool using the Qiagen DNeasy PowerSoil Pro kit for the mouse experiments and Qiagen DNeasy PowerSoil for the cultivar experiments. Extracted DNA was quantified using the Quant-iTTM PicoGreen dsDNA assay kit (Thermo Fisher Scientific). Shotgun libraries were generated from 7.5 ng DNA using IDT for Illumina unique dual indexes and Illumina DNA Prep Library Prep kit for the mouse experiments and Illumina XT for the cultivar experiments at 1:4 scale reaction volume. Library success was assessed by Quant-iT PicoGreen dsDNA assay. Equal volumes of library were pooled from every sample and sequenced using a 300 cycle Nano kit on the Illumina MiSeq. Libraries were then repooled based on the demultiplexing statistics of the MiSeq Nano run. Final libraries were QCed on the Agilent BioAnalyzer to check the size distribution and absence of additional adaptor fragments. Libraries were sequenced on an Illumina Novaseq 6000 v1.5 flow cell for the mouse experiments and Illumina HiSeq 2500 v4 flow cell for the cultivar experiments, producing 2x150 bp paired-end reads. Extraction blanks and nucleic acid-free water were processed along with experimental samples to empirically assess environmental and reagent contamination. A laboratory-generated mock community consisting of DNA from Vibrio campbellii and Lambda phage was included as a positive sequencing control.

Shotgun metagenomic data were analyzed using Sunbeam version 2.1.1 (71). Quality control steps were performed by the default workflows in Sunbeam, which include removing adapters, reads of low sequence complexity and host-derived sequences. The abundance of bacteria was estimated using Kraken (72). Reads were mapped to the KEGG database to estimate the abundance of bacterial gene orthologs (73). Contigs were assembled from the samples in the FARMM dataset using MegaHit version 1.1.3 (74). The genes were predicted from the contigs using Prodigal version 2.6.3 (75). The predicted gene sequences were aligned against KEGG database using diamond aligner (76).

Within sample diversity was assessed using Shannon diversity metric. Between sample similarity was assessed by Bray-Curtis distance. Community-level differences between sample groups were assessed using the PERMANOVA test. Differences in bacterial abundance or gene orthologs were assessed using linear models on log10 transformed relative abundances or RPKM values. Only bacteria with 1% mean relative abundance in at least one comparison are tested. P-values from multiple testing procedures will be corrected to control for a specified false discovery rate using Benjamini-Hochberg method. A cutoff of 20% of the total microbiota during the recovery phase, based on shotgun sequencing, was used for analysis of *K. pneumoniae* high and low subcategorization. Once subcategorized, ammonia and urea levels were compared during the three dietary phases for each subgroup.

Metabolite quantification

Amino acids were quantified as previously described using a Waters Acquity uPLC System with an AccQ-Tag Ultra C18 1.7 µm 2.1x100mm column and a Photodiode Detector Array (35). Fecal samples were homogenized in methanol (5 µL/mg stool) and centrifuged twice at 13,000g for 5 minutes. Amino acids in the supernatant were derivatized using the Waters AccQ-Tag Ultra Amino Acid Derivatization Kit (Waters Corporation, Milford, MA) and analyzed using the UPLC AAA H-

Class Application Kit (Waters Corporation, Milford, MA) according to manufacturer's instructions. All chemicals and reagents used were mass spectrometry grade.

Stool urea quantification was performed with the Quantichrom urea kit as follows: stool samples were homogenized in 10µL of ddH_2O per mg stool. Solid debris was removed via centrifugation at 2500 x g for 10 minutes. Supernatant was tested for urea quantity per manufacturer protocol.

Stool metabolites were quantified using ^{1}H NMR-based metabolomics as follows: approximately 50 mg of wet stool sample was weighed and extracted using phosphate buffered solution containing 50% D_2O with 0.29 mM TMSP as internal standard. The ^{1}H spectra of extracts were acquired at 298 K using a Bruker Avance NEO 600 MHz spectrometer equipped with a SampleJet sample changer (Bruker Biospin, Rheinstetten, Germany). The noesygppr1d pulse sequence was used for recording ^{1}H 1D NMR experiments with pre-saturation water suppression during relaxation and mixing time. All ^{1}H NMR spectra were processed automatically with Chenomx NMR Suite (Chenomx Inc, Edmonton, Alberta, Canada, version 9.05), then each spectrum was checked and adjusted manually for phase and baseline. Metabolites were identified and spectral fit using an in-house metabolite library. Metabolite concentrations were calculated according to internal standard for further statistical analysis.

Quantification and Statistical Analysis

Prism Software (GraphPad, Inc.) was used to perform indicated statistical analyses. Statistical tests and p-values considered significant are noted in respective figure legends.

Study Approval

All animal studies were conducted in accordance with ethical regulations under protocols approved by the University of Pennsylvania Institutional Animal Care and Use and Biosafety Committees. The University of Pennsylvania Institutional Review Board (IRB) approved the

FARMM study protocol and considered it exempt from clinical trial registration requirement. Written informed consent was received prior to participation.

Resource Availability

Further information and requests for resources should be directed to Gary D. Wu (gdwu@pennmedicine.upenn.edu).

Materials Availability

Reagents and strains generated from this study will be made available upon reasonable request with appropriate materials transfer agreement.

Data and Code Availability

Shotgun sequencing data from the FARMM study is publicly available as previously reported in the Sequence Read Archive (SRA): PRJNA675301.

Shotgun sequencing data from this paper is publicly available in the SRA: PRJNA97602 and PRJNA1065816.

Data values presented in figures are provided in Supporting Data Values file.

Author Contributions

A.L.H, L.C.H., J.L., M.G., and G.D.W. designed, and analyzed the bacterial culture, human fecal testing, and mouse studies; A.L.H, L.C.H., J.L. performed the bacterial culture and mouse studies. E.S.F., J.F., L.L., and G.D.W designed the bioreactor studies; E.S.F and J.F. performed the bioreactor studies; C.T., V.T., and K.B performed the sequencing analysis; F.H. and A.D.P performed and analyzed the NMR metabolite quantification data. A.L.H, M.G., and G.D.W. wrote the manuscript.

Acknowledgements

This work was supported by the Division of Gastroenterology and Hepatology at the Hospital of the University of Pennsylvania and funded by the NIH P30 Center for Molecular Studies in Digestive and Liver Diseases, NIH R35GM139541, the Crohn's and Colitis Foundation. We also acknowledge the assistance of the PennCHOP Microbiome Program, and the University of Pennsylvania Gnotobiotic Facility. We thank the Microbial Culture & Metabolomics Core of the PennCHOP Microbiome Program and the Center for Molecular Studies in Digestive and Liver Diseases (NIH P30DK050306), the Penn Molecular Pathology and Imaging Core (NIH P30 DK050306), the Penn Host Microbial Analytic and Repository Core (H-MARC), and the Penn Center for Nutritional Science & Medicine (PenNSAM) for their technical expertise. A.L.H. is supported by the Division of Gastroenterology basic science T32 (DK007066). We thank Lillian Chau, Lindsay Herman, and Dylan Curry for their technical expertise and assistance.

References

1. Bajaj JS, Kamath PS, Reddy KR. The Evolving Challenge of Infections in Cirrhosis. Longo DL, ed. *N Engl J Med*. 2021;384(24):2317-2330. doi:10.1056/NEJMra2021808

2. Wiest R, Lawson M, Geuking M. Pathological bacterial translocation in liver cirrhosis. *Journal of Hepatology*. 2014;60(1):197-209. doi:10.1016/j.jhep.2013.07.044

3. McMahon S, Sahasrabhojane P, Kim J, et al. Contribution of the Oral and Gastrointestinal Microbiomes to Bloodstream Infections in Leukemia Patients. Claesen J, ed. *Microbiol Spectr*. 2023;11(3):e00415-23. doi:10.1128/spectrum.00415-23

4. Taur Y, Xavier JB, Lipuma L, et al. Intestinal Domination and the Risk of Bacteremia in Patients Undergoing Allogeneic Hematopoietic Stem Cell Transplantation. *Clinical Infectious Diseases*. 2012;55(7):905-914. doi:10.1093/cid/cis580

5. Freedberg DE, Zhou MJ, Cohen ME, et al. Pathogen colonization of the gastrointestinal microbiome at intensive care unit admission and risk for subsequent death or infection. *Intensive Care Med*. 2018;44(8):1203-1211. doi:10.1007/s00134-018-5268-8

6. Dalal SR, Chang EB. The microbial basis of inflammatory bowel diseases. *J Clin Invest*. 2014;124(10):4190-4196. doi:10.1172/JCI72330

7. Seksik P. Alterations of the dominant faecal bacterial groups in patients with Crohn's disease of the colon. *Gut*. 2003;52(2):237-242. doi:10.1136/gut.52.2.237

8. Bajaj JS, Heuman DM, Hylemon PB, et al. Altered profile of human gut microbiome is associated with cirrhosis and its complications. *Journal of Hepatology*. 2014;60(5):940-947. doi:10.1016/j.jhep.2013.12.019

9. Adelman MW, Woodworth MH, Langelier C, et al. The gut microbiome's role in the development, maintenance, and outcomes of sepsis. *Crit Care*. 2020;24(1):278. doi:10.1186/s13054-020-02989-1

10. Liu Z, Li N, Fang H, et al. Enteric dysbiosis is associated with sepsis in patients. *FASEB j*. 2019;33(11):12299-12310. doi:10.1096/fj.201900398RR

11. Schlechte J, Zucoloto AZ, Yu I ling, et al. Dysbiosis of a microbiota–immune metasystem in critical illness is associated with nosocomial infections. *Nat Med*. 2023;29(4):1017-1027. doi:10.1038/s41591-023-02243-5

12. Lupp C, Robertson ML, Wickham ME, et al. Host-Mediated Inflammation Disrupts the Intestinal Microbiota and Promotes the Overgrowth of Enterobacteriaceae. *Cell Host & Microbe*. 2007;2(3):204. doi:10.1016/j.chom.2007.08.002

13. Shin NR, Whon TW, Bae JW. Proteobacteria: microbial signature of dysbiosis in gut microbiota. *Trends in Biotechnology*. 2015;33(9):496-503. doi:10.1016/j.tibtech.2015.06.011

14. Peterson DA, Frank DN, Pace NR, Gordon JI. Metagenomic Approaches for Defining the Pathogenesis of Inflammatory Bowel Diseases. *Cell Host & Microbe*. 2008;3(6):417-427. doi:10.1016/j.chom.2008.05.001

15. Potruch A, Schwartz A, Ilan Y. The role of bacterial translocation in sepsis: a new target for therapy. *Therap Adv Gastroenterol*. 2022;15:175628482210942. doi:10.1177/17562848221094214

16. O'Boyle CJ, MacFie J, Mitchell CJ, Johnstone D, Sagar PM, Sedman PC. Microbiology of bacterial translocation in humans. *Gut*. 1998;42(1):29-35. doi:10.1136/gut.42.1.29

17. Lee CC, Feng Y, Yeh YM, et al. Gut Dysbiosis, Bacterial Colonization and Translocation, and Neonatal Sepsis in Very-Low-Birth-Weight Preterm Infants. *Front Microbiol*. 2021;12:746111. doi:10.3389/fmicb.2021.746111

18. Worby CJ, Schreiber HL, Straub TJ, et al. Longitudinal multi-omics analyses link gut microbiome dysbiosis with recurrent urinary tract infections in women. *Nat Microbiol*. 2022;7(5):630-639. doi:10.1038/s41564-022-01107-x

19. Schmitz JM, Tonkonogy SL, Dogan B, et al. Murine Adherent and Invasive *E. coli* Induces Chronic Inflammation and Immune Responses in the Small and Large Intestines of Monoassociated IL-10-/- Mice Independent of Long Polar Fimbriae Adhesin A. *Inflammatory Bowel Diseases*. 2019;25(5):875-885. doi:10.1093/ibd/izy386

20. Federici S, Kredo-Russo S, Valdés-Mas R, et al. Targeted suppression of human IBD-associated gut microbiota commensals by phage consortia for treatment of intestinal inflammation. *Cell*. 2022;185(16):2879-2898.e24. doi:10.1016/j.cell.2022.07.003

21. Lewis JD, Sandler RS, Brotherton C, et al. A Randomized Trial Comparing the Specific Carbohydrate Diet to a Mediterranean Diet in Adults With Crohn's Disease. *Gastroenterology*. 2021;161(3):837-852.e9. doi:10.1053/j.gastro.2021.05.047

22. Suskind DL, Cohen SA, Brittnacher MJ, et al. Clinical and Fecal Microbial Changes With Diet Therapy in Active Inflammatory Bowel Disease. *Journal of Clinical Gastroenterology*. 2018;52(2):155-163. doi:10.1097/MCG.0000000000000772

23. Baxter NT, Schmidt AW, Venkataraman A, Kim KS, Waldron C, Schmidt TM. Dynamics of Human Gut Microbiota and Short-Chain Fatty Acids in Response to Dietary Interventions with Three Fermentable Fibers. Blaser MJ, ed. *mBio*. 2019;10(1):e02566-18. doi:10.1128/mBio.02566-18

24. Johnson AJ, Vangay P, Al-Ghalith GA, et al. Daily Sampling Reveals Personalized Diet-Microbiome Associations in Humans. *Cell Host & Microbe*. 2019;25(6):789-802.e5. doi:10.1016/j.chom.2019.05.005

25. Wu GD, Chen J, Hoffmann C, et al. Linking Long-Term Dietary Patterns with Gut Microbial Enterotypes. *Science*. 2011;334(6052):105-108. doi:10.1126/science.1208344

26. Sonnenburg ED, Sonnenburg JL. Starving our Microbial Self: The Deleterious Consequences of a Diet Deficient in Microbiota-Accessible Carbohydrates. *Cell Metabolism*. 2014;20(5):779-786. doi:10.1016/j.cmet.2014.07.003

27. Sonnenburg ED, Smits SA, Tikhonov M, Higginbottom SK, Wingreen NS, Sonnenburg JL. Diet-induced extinctions in the gut microbiota compound over generations. *Nature*. 2016;529(7585):212-215. doi:10.1038/nature16504

28. Fischbach MA, Sonnenburg JL. Eating For Two: How Metabolism Establishes Interspecies Interactions in the Gut. *Cell Host & Microbe*. 2011;10(4):336-347. doi:10.1016/j.chom.2011.10.002

29. Reese AT, Pereira FC, Schintlmeister A, et al. Microbial nitrogen limitation in the mammalian large intestine. *Nat Microbiol*. 2018;3(12):1441-1450. doi:10.1038/s41564-018-0267-7

30. Holmes AJ, Chew YV, Colakoglu F, et al. Diet-Microbiome Interactions in Health Are Controlled by Intestinal Nitrogen Source Constraints. *Cell Metab*. 2017;25(1):140-151. doi:10.1016/j.cmet.2016.10.021

31. Zeng X, Xing X, Gupta M, et al. Gut bacterial nutrient preferences quantified in vivo. *Cell*. 2022;185(18):3441-3456.e19. doi:10.1016/j.cell.2022.07.020

32. Wostmann BS. THE GERMFREE ANIMAL IN NUTRITIONAL STUDIES. *Annu Rev Nutr*. 1981;1(1):257-279. doi:10.1146/annurev.nu.01.070181.001353

33. Tanes C, Bittinger K, Gao Y, et al. Role of dietary fiber in the recovery of the human gut microbiome and its metabolome. *Cell Host & Microbe*. 2021;29(3):394-407.e5. doi:10.1016/j.chom.2020.12.012

34. Winter SE, Lopez CA, Bäumler AJ. The dynamics of gut-associated microbial communities during inflammation. *EMBO Rep*. 2013;14(4):319-327. doi:10.1038/embor.2013.27

35. Ni J, Shen TCD, Chen EZ, et al. A role for bacterial urease in gut dysbiosis and Crohn's disease. *Sci Transl Med*. 2017;9(416):eaah6888. doi:10.1126/scitranslmed.aah6888

36. Firrman J, Liu L, Mahalak K, et al. Comparative analysis of the gut microbiota cultured in vitro using a single colon versus a 3-stage colon experimental design. *Appl Microbiol Biotechnol*. 2021;105(8):3353-3367. doi:10.1007/s00253-021-11241-x

37. Wang J, Yan D, Dixon R, Wang YP. Deciphering the Principles of Bacterial Nitrogen Dietary Preferences: a Strategy for Nutrient Containment. Harwood CS, ed. *mBio*. 2016;7(4):e00792-16. doi:10.1128/mBio.00792-16

38. Lasaro M, Liu Z, Bishar R, et al. Escherichia coli Isolate for Studying Colonization of the Mouse Intestine and Its Application to Two-Component Signaling Knockouts. *J Bacteriol*. 2014;196(9):1723-1732. doi:10.1128/JB.01296-13

39. Shen TCD, Chehoud C, Ni J, et al. Dietary Regulation of the Gut Microbiota Engineered by a Minimal Defined Bacterial Consortium. Rawls JF, ed. *PLoS ONE*. 2016;11(5):e0155620. doi:10.1371/journal.pone.0155620

40. Patnode ML, Beller ZW, Han ND, et al. Interspecies Competition Impacts Targeted Manipulation of Human Gut Bacteria by Fiber-Derived Glycans. *Cell*. 2019;179(1):59-73.e13. doi:10.1016/j.cell.2019.08.011

41. Desai MS, Seekatz AM, Koropatkin NM, et al. A Dietary Fiber-Deprived Gut Microbiota Degrades the Colonic Mucus Barrier and Enhances Pathogen Susceptibility. *Cell*. 2016;167(5):1339-1353.e21. doi:10.1016/j.cell.2016.10.043

42. Llewellyn SR, Britton GJ, Contijoch EJ, et al. Interactions Between Diet and the Intestinal Microbiota Alter Intestinal Permeability and Colitis Severity in Mice. *Gastroenterology*. 2018;154(4):1037-1046.e2. doi:10.1053/j.gastro.2017.11.030

43. Okayasu I, Hatakeyama S, Yamada M, Ohkusa T, Inagaki Y, Nakaya R. A novel method in the induction of reliable experimental acute and chronic ulcerative colitis in mice. *Gastroenterology*. 1990;98(3):694-702. doi:10.1016/0016-5085(90)90290-H

44. Shen TCD, Albenberg L, Bittinger K, et al. Engineering the gut microbiota to treat hyperammonemia. *J Clin Invest*. 2015;125(7):2841-2850. doi:10.1172/JCI79214

45. Liu Y, Chen H, Van Treuren W, Hou BH, Higginbottom SK, Dodd D. Clostridium sporogenes uses reductive Stickland metabolism in the gut to generate ATP and produce circulating metabolites. *Nat Microbiol*. 2022;7(5):695-706. doi:10.1038/s41564-022-01109-9

46. Nisman B. The Stickland reaction. *Bacteriol Rev*. 1954;18(1):16-42. doi:10.1128/br.18.1.16-42.1954

47. *Physiology of the Gastrointestinal Tract*. Elsevier; 2012. doi:10.1016/C2009-1-64521-4

48. Delbaere K, Roegiers I, Bron A, et al. The small intestine: dining table of host–microbiota meetings. *FEMS Microbiology Reviews*. 2023;47(3):fuad022. doi:10.1093/femsre/fuad022

49. Jeanes A, Hodge J, eds. *Physiological Effects of Food Carbohydrates*. Vol 15. AMERICAN CHEMICAL SOCIETY; 1975. doi:10.1021/bk-1975-0015

50. Chang DE, Smalley DJ, Tucker DL, et al. Carbon nutrition of *Escherichia coli* in the mouse intestine. *Proc Natl Acad Sci USA*. 2004;101(19):7427-7432. doi:10.1073/pnas.0307888101

51. Fabich AJ, Jones SA, Chowdhury FZ, et al. Comparison of Carbon Nutrition for Pathogenic and Commensal *Escherichia coli* Strains in the Mouse Intestine. *Infect Immun*. 2008;76(3):1143-1152. doi:10.1128/IAI.01386-07

52. Hudson AW, Barnes AJ, Bray AS, Ornelles DA, Zafar MA. Klebsiella pneumoniae L- Fucose Metabolism Promotes Gastrointestinal Colonization and Modulates Its Virulence Determinants. Raffatellu M, ed. *Infect Immun*. 2022;90(10):e00206-22. doi:10.1128/iai.00206-22

53. Reimer RA, Soto-Vaca A, Nicolucci AC, et al. Effect of chicory inulin-type fructan–containing snack bars on the human gut microbiota in low dietary fiber consumers in a randomized crossover trial. *The American Journal of Clinical Nutrition*. 2020;111(6):1286-1296. doi:10.1093/ajcn/nqaa074

54. Tandon D, Haque MM, Gote M, et al. A prospective randomized, double-blind, placebo-controlled, dose-response relationship study to investigate efficacy of fructo-oligosaccharides (FOS) on human gut microflora. *Sci Rep*. 2019;9(1):5473. doi:10.1038/s41598-019-41837-3

55. Wu GD, Compher C, Chen EZ, et al. Comparative metabolomics in vegans and omnivores reveal constraints on diet-dependent gut microbiota metabolite production. *Gut*. 2016;65(1):63-72. doi:10.1136/gutjnl-2014-308209

56. Wastyk HC, Fragiadakis GK, Perelman D, et al. Gut-microbiota-targeted diets modulate human immune status. *Cell*. 2021;184(16):4137-4153.e14. doi:10.1016/j.cell.2021.06.019

57. Sorbara MT, Dubin K, Littmann ER, et al. Inhibiting antibiotic-resistant Enterobacteriaceae by microbiota-mediated intracellular acidification. *Journal of Experimental Medicine*. 2019;216(1):84-98. doi:10.1084/jem.20181639

58. Hryckowian AJ, Van Treuren W, Smits SA, et al. Microbiota-accessible carbohydrates suppress Clostridium difficile infection in a murine model. *Nat Microbiol*. 2018;3(6):662-669. doi:10.1038/s41564-018-0150-6

59. Gipson KS, Nickerson KP, Drenkard E, et al. The Great ESKAPE: Exploring the Crossroads of Bile and Antibiotic Resistance in Bacterial Pathogens. Ottemann KM, ed. *Infect Immun*. 2020;88(10):e00865-19. doi:10.1128/IAI.00865-19

60. Bogatyrev SR, Rolando JC, Ismagilov RF. Self-reinoculation with fecal flora changes microbiota density and composition leading to an altered bile-acid profile in the mouse small intestine. *Microbiome*. 2020;8(1):19. doi:10.1186/s40168-020-0785-4

61. Martin RM, Cao J, Brisse S, et al. Molecular Epidemiology of Colonizing and Infecting Isolates of Klebsiella pneumoniae. Castanheira M, ed. *mSphere*. 2016;1(5):e00261-16. doi:10.1128/mSphere.00261-16

62. Armstrong HK, Bording-Jorgensen M, Santer DM, et al. Unfermented β-fructan Fibers Fuel Inflammation in Select Inflammatory Bowel Disease Patients. *Gastroenterology*. 2023;164(2):228-240. doi:10.1053/j.gastro.2022.09.034

63. Kuffa P, Pickard JM, Campbell A, et al. Fiber-deficient diet inhibits colitis through the regulation of the niche and metabolism of a gut pathobiont. *Cell Host & Microbe*. 2023;31(12):2007-2022.e12. doi:10.1016/j.chom.2023.10.016

64. Chen AI, Albicoro FJ, Zhu J, Goulian M. Effects of Regulatory Network Organization and Environment on PmrD Connector Activity and Polymyxin Resistance in *Klebsiella pneumoniae* and *Escherichia coli*. *Antimicrob Agents Chemother*. 2021;65(3). doi:10.1128/AAC.00889-20

65. Huang TW, Lam I, Chang HY, Tsai SF, Palsson BO, Charusanti P. Capsule deletion via a λ-Red knockout system perturbs biofilm formation and fimbriae expression in Klebsiella pneumoniae MGH 78578. *BMC Res Notes*. 2014;7(1):13. doi:10.1186/1756-0500-7-13

66. Liu L, Firrman J, Tanes C, et al. Establishing a mucosal gut microbial community in vitro using an artificial simulator. *PLoS One*. 2018;13(7):e0197692. doi:10.1371/journal.pone.0197692

67. Velazquez EM, Nguyen H, Heasley KT, et al. Endogenous Enterobacteriaceae underlie variation in susceptibility to Salmonella infection. *Nat Microbiol*. 2019;4(6):1057-1064. doi:10.1038/s41564-019-0407-8

68. Cooper HS, Murthy SN, Shah RS, Sedergran DJ. Clinicopathologic study of dextran sulfate sodium experimental murine colitis. *Lab Invest*. 1993;69(2):238-249.

69. Suzuki R, Kohno H, Sugie S, Nakagama H, Tanaka T. Strain differences in the susceptibility to azoxymethane and dextran sodium sulfate-induced colon carcinogenesis in mice. *Carcinogenesis*. 2005;27(1):162-169. doi:10.1093/carcin/bgi205

70. Kennedy RJ, Hoper M, Deodhar K, Erwin PJ, Kirk SJ, Gardiner KR. Interleukin 10-deficient colitis: new similarities to human inflammatory bowel disease. *British Journal of Surgery*. 2002;87(10):1346-1351. doi:10.1046/j.1365-2168.2000.01615.x

71. Clarke EL, Taylor LJ, Zhao C, et al. Sunbeam: an extensible pipeline for analyzing metagenomic sequencing experiments. *Microbiome*. 2019;7(1):46. doi:10.1186/s40168-019-0658-x

72. Wood DE, Salzberg SL. Kraken: ultrafast metagenomic sequence classification using exact alignments. *Genome Biol*. 2014;15(3):R46. doi:10.1186/gb-2014-15-3-r46

73. Ogata H, Goto S, Sato K, Fujibuchi W, Bono H, Kanehisa M. KEGG: Kyoto Encyclopedia of Genes and Genomes. *Nucleic Acids Res*. 1999;27(1):29-34. doi:10.1093/nar/27.1.29

74. Li D, Luo R, Liu CM, et al. MEGAHIT v1.0: A fast and scalable metagenome assembler driven by advanced methodologies and community practices. *Methods*. 2016;102:3-11. doi:10.1016/j.ymeth.2016.02.020

75. Hyatt D, Chen GL, Locascio PF, Land ML, Larimer FW, Hauser LJ. Prodigal: prokaryotic gene recognition and translation initiation site identification. *BMC Bioinformatics*. 2010;11:119. doi:10.1186/1471-2105-11-119

76. Buchfink B, Reuter K, Drost HG. Sensitive protein alignments at tree-of-life scale using DIAMOND. *Nat Methods*. 2021;18(4):366-368. doi:10.1038/s41592-021-01101-x

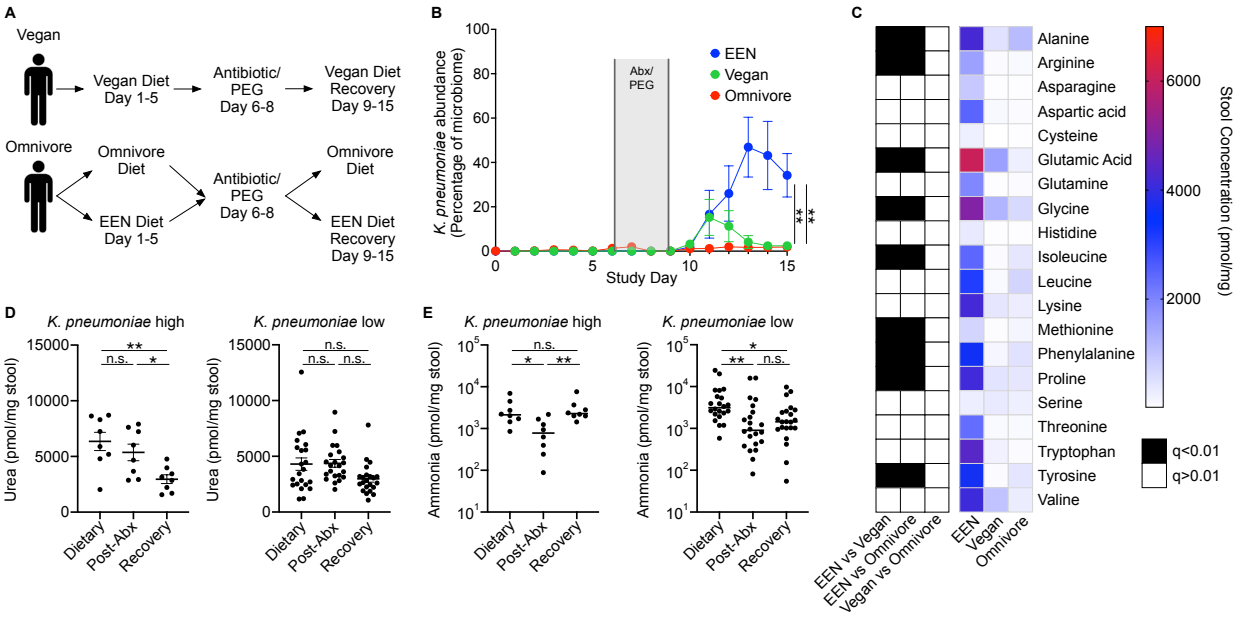

Figure 1. A defined formula diet favors *K. pneumoniae* growth in human subjects. **A**. Diagram of the FARMM study design. Patients were randomized to an FF diet (EEN) or an omnivore diet; a third group remained on a vegan diet throughout the study. Recovery of the microbiome was monitored after antibiotic (abx) and polyethylene glycol (PEG) depletion. **B**. Relative abundance of *K. pneumoniae* as a percentage of the microbiome determined via shotgun metagenomic sequencing, stratified by dietary group. **C**. Heat map of average stool amino acid concentrations during the microbiome recovery phase (Day 14) of the FARMM study, stratified by diet. Black boxes denote statistically significant difference of amino acid concentration between indicated dietary groups. **D and E**. Quantification of stool urea (**D**) and ammonia (**E**) at each phase of the FARMM study, from individuals with high or low relative abundance of *K. pneumoniae* (defined as greater than 20% *K. pneumoniae* by relative abundance during the recovery phase). Data presented as mean ± SEM, n=10 subjects per dietary group. Results of one-way ANOVA with Holm-Sidak correction for multiple comparisons (**B,** comparing EEN vs Omnivore and EEN vs Vegan groups on Day 15; **D**), multiple Mann-Whitney tests with FDR method of Benjamini, Krueger, Yokutieli (**C**), or Kruskal-Wallis test with Dunn's multiple comparisons test (**E**), n.s., not significant, *p<0.05, **p<0.01.

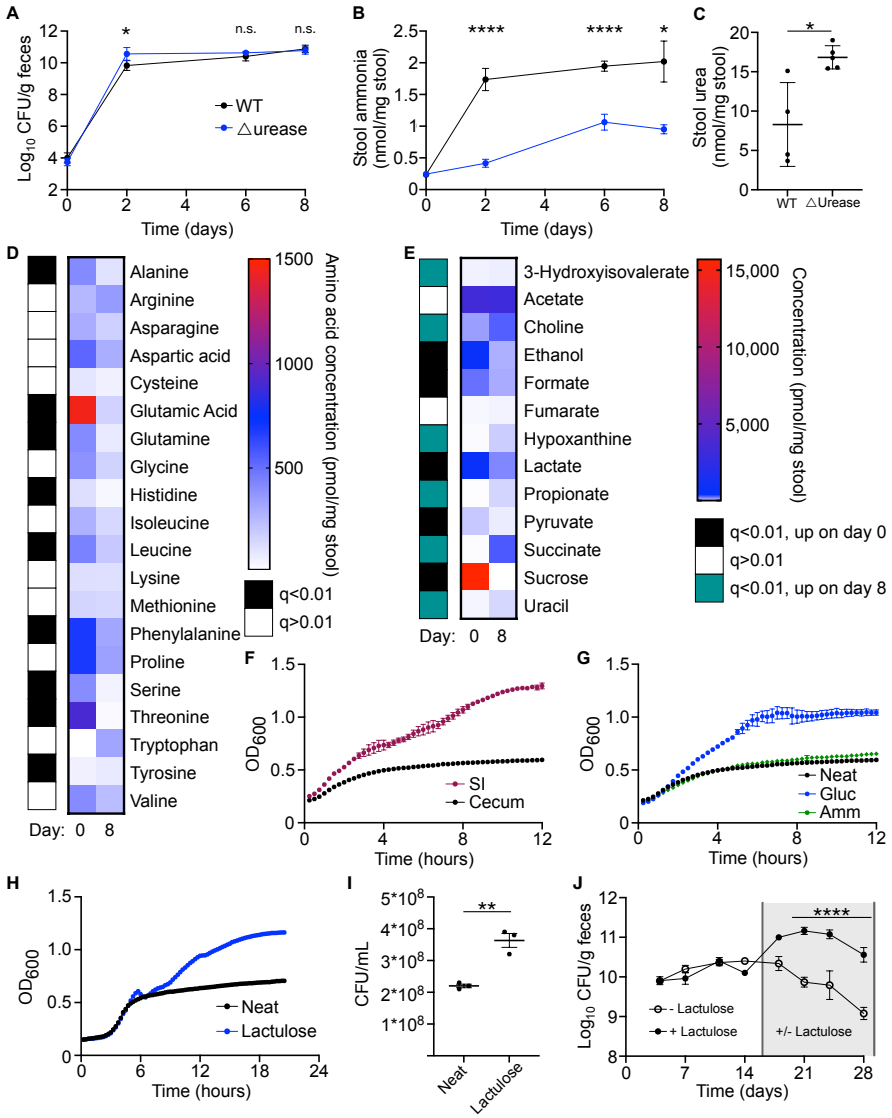

Figure 2. *K. pneumoniae* colonization is limited by carbon source availability and alters the nitrogen environment in the gut. **A-E**. Germ-free mice were colonized with WT or △urease *K. pneumoniae* and serial stool collections performed throughout the 1-week study. Fecal CFU (**A**) and stool ammonia (**B**) were monitored for 1 week after colonization. Fecal urea (**C**) was tested at day 8. Stool amino acid levels (**D**) and metabolites (**E**) were quantified from stool before (day 0) and after (day 8) WT K. *pneumoniae* colonization. **F.** Growth of WT *K. pneumoniae* in small intestine (SI) or cecal extract of mice monitored via OD_{600}. **G and H**. Growth in cecal extract supplemented with ammonia or glucose (**G**), or lactulose (**H and I**) quantified by OD_{600} and CFU (**I**). Data for neat cecal extract are presented in both **F and G** for reference. **J**. Mice colonized with *K. pneumoniae* were subsequently treated with lactulose in the drinking water or water-only control. Data presented as mean ± SEM (**A and J**) or mean ± SD (**B, C**, **and F-I**); n=4-5 mice per group (**A-E, J**) or n=3 wells per group (**F-I**). Data represents combined results from two independent experiments (**A-E**) or are a single experiment representative of three independent experiments (**F-J**). Results of multiple unpaired t-tests with Benjamini Hochberg multiple corrections (**D, E**), with Bonferroni multiple corrections (**A, B, J**) or unpaired t-test (**C, I**), n.s. not significant, *p<0.05, **p<0.01, ****p<0.001.

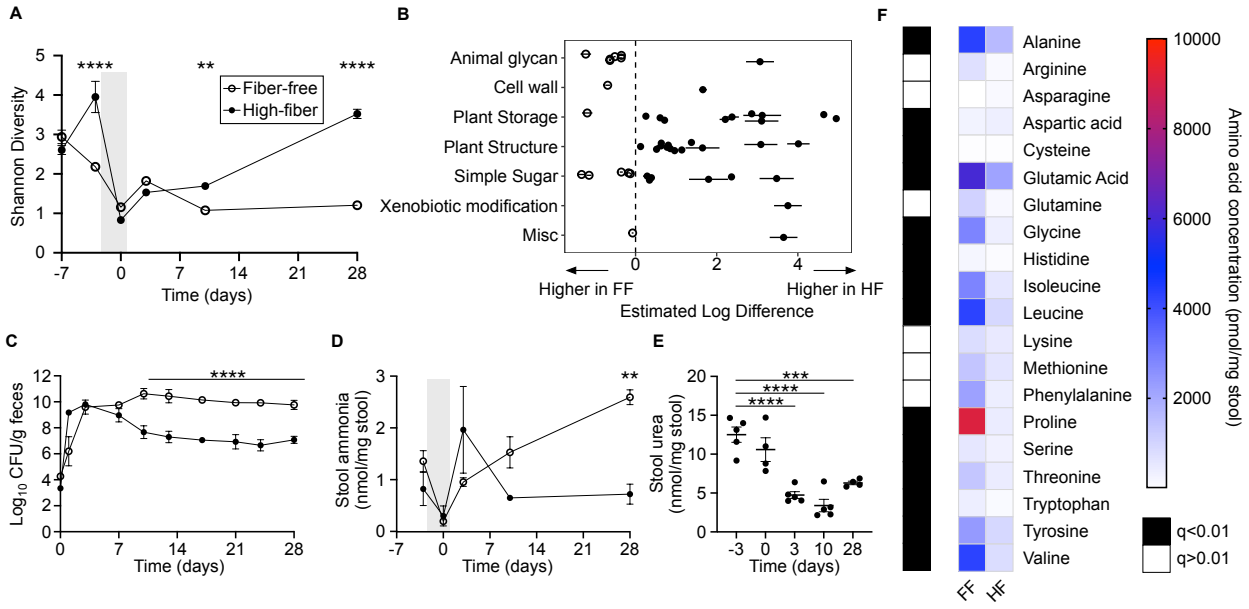

Figure 3. Complex carbohydrates increase microbiome diversity and reduce *K. pneumoniae* colonization after antibiotic depletion. **A-F**. Mice were provided a fiber-free (FF) or high-fiber (HF) diet (starting at day -7), treated with oral antibiotics (day -3 to 0, grey shading), and gavaged with *K. pneumoniae* (day 0). Serial stool samples were subjected to analysis as follows: **A.** Shannon alpha-diversity of stool microbiome from mice provided a fiber-free (FF) or high-fiber (HF) diet including antibiotic treatment period (grey shading) and recovery, as determined by shotgun metagenomic sequencing. **B.** Glycoside hydrolase (GH) genes with significantly different abundances between FF and FH diets four-weeks after gavage with K. pneumoniae grouped by substrate type. Open circles represent genes with higher levels in FF diet and closed circles represent genes with higher levels in HF diet. **C.** *K. pneumoniae* fecal CFU of mice on FF (open circles) or HF (closed circles) diets measured four weeks after *K. pneumoniae* gavage. **D**. Stool ammonia was quantified before and after antibiotic treatment (grey shading) and *K. pneumoniae* gavage from mice subjected to FF (open circles) or HF (closed circles) diets. **E.** Stool urea levels were quantified from mice provided a FF diet. **F**. Heat map of amino acid concentrations from mice on an FF or HF diet after colonization with *K. pneumoniae*. Data are presented as mean ± SD (**A-E**), n= 5 mice per group. Data representative of two to three independent experiments (**C-F**). Results of multiple t-test with Bonferroni correction for multiple comparisons (**A, C, D**), one-way ANOVA with Bonferroni correction for multiple comparisons (**E**), or multiple Mann-Whitney tests with FDR method of Benjamini, Krueger, Yokutieli (**F**), n.s. not significant, **p<0.01, ***p<0.001, ****p<0.0001.

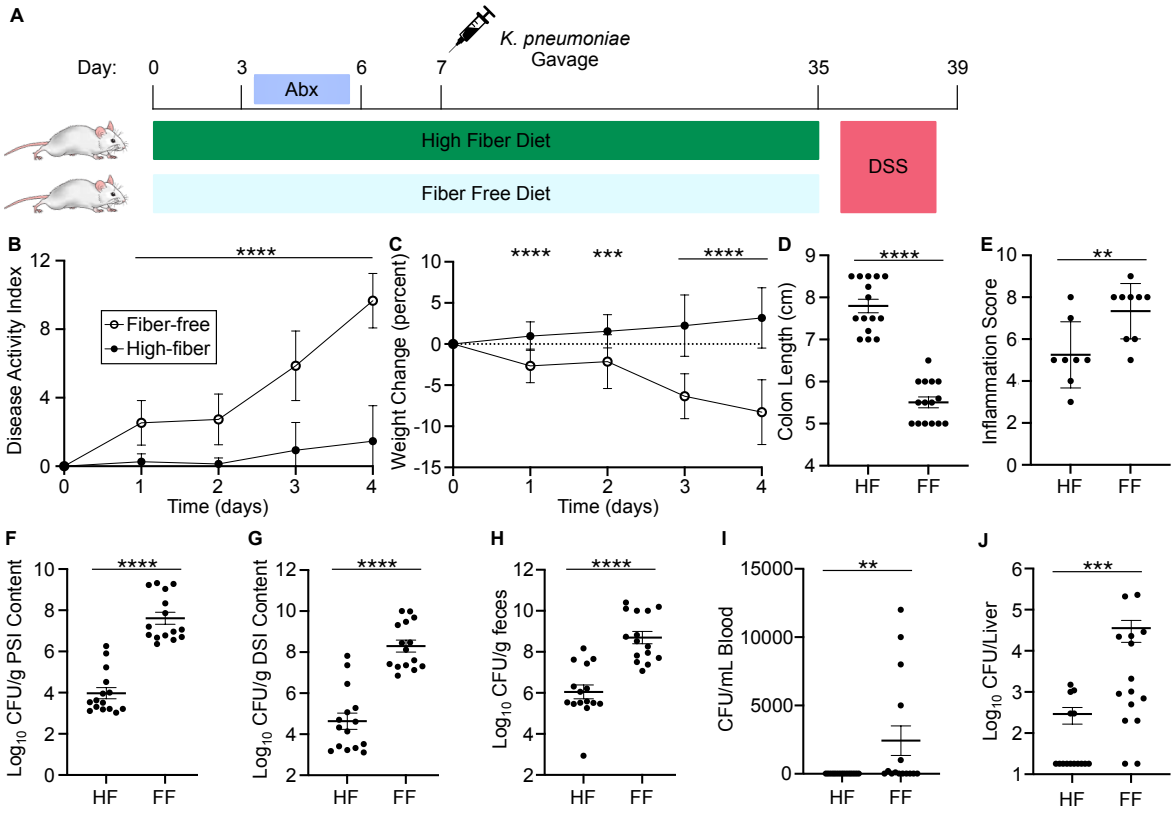

Figure 4. High fiber diet protects against DSS colitis and *K. pneumoniae* dissemination from the microbiota. **A.** Diagram of experimental design. Mice were placed on a HF or FF diet and colonized with WT *K. pneumoniae* after antibiotic pretreatment followed by treatment with 5% DSS in the drinking water. **B and C.** Disease activity (**B**) and weight change (**C**) were monitored during DSS treatment. After 4 days of treatment, mice were euthanized. **D.** Colon length was quantified. **E.** Colon tissue was microscopically scored for evidence of inflammation. **F-J** CFU was quantified in the proximal small intestine (**F**), distal small intestine (**G**), feces (**H**), blood (**I**), and liver (**J**). Data are presented as mean ± SD. Results are a combination of three independent experiments (**B, C, and F-J**; n=15 mice per group) or a combination of two independent experiments (**E**; n= 8-9 mice per group). Results of multiple unpaired t-tests with Bonferroni multiple correction (**B and C**), unpaired t-test (**D-H**) or Mann-Whitney test (**I and J**), **p<0.01, ***p<0.001, ****p<0.0001.